DOI: 10.15514/ISPRAS-2022-34(6)-15

Effect of relative longitudinal spacing on the dynamic behavior of two interacting ships in head waves

R. Ali, ORCID: 0000-0003-0591-6221 <ramimamdouhali@gmail.com>

State Marine Technical University (SMTU),
Lotsmanskaya st.3, Saint-Petersburg, 190121, Russia

Abstract. The influence of relative longitudinal position on the frequency characteristics of two interacting ships floating stationary in close proximity in head waves and shallow water is investigated in this paper. A CFD approach has been adopted to simulate the dynamic behavior of the interacting ships. The numerical simulation for “Aleksey Kosygin” and “Novgorod” ships floating on head waves at a small relative transverse distance $\boldsymbol{\eta = 1.3}$ was carried out using two scaled models. The effect of longitudinal separation on the frequency characteristics of both ships was studied. Heave, roll, and pitch RAOs for various cases were analyzed, and recommendations for relative longitudinal positions were made on the basis of the present analysis.

Keywords: Lightering operation; Hydrodynamic Interaction; ship motions; RANS; CFD; OpenFOAM

For citation: Ali R. Effect of relative longitudinal spacing on the dynamic behavior of two interacting ships in head waves. Trudy ISP RAN/Proc. ISP RAS, vol. 34, issue 6, 2022. pp. 185-196. DOI: 10.15514/ISPRAS-2022-34(6)-15

Влияние относительного продольного расстояния на динамическое поведение двух взаимодействующих судов при встречном волнении

Рами Али, ORCID: 0000-0003-0591-6221 <ramimamdouhali@gmail.com>

Санкт-Петербургский Государственный морской технический университет,
190121, Россия, Санкт-Петербург, ул. Лоцманская, 3

Аннотация. В работе исследуется влияние взаимного продольного положения на частотные характеристики двух взаимодействующих судов, плавающих неподвижно в непосредственной близости на встречном волнении и мелководье. Подход CFD был принят для моделирования динамического поведения взаимодействующих судов. Численное моделирование судов «Алексей Косыгин» и «Новгород», плавающих на встречных волнах при малом относительном поперечном расстоянии η=1,3, проводилось с использованием двух масштабных моделей. Исследовано влияние продольного расстояния на частотные характеристики обоих судов. Были проанализированы АЧХ вертикальной, килевой и бортовой качки для различных случаев, и на основе настоящего анализа были даны рекомендации по относительному продольному положению.

Ключевые слова: лихтеровка; гидродинамическое взаимодействие; качка судов; RANS; CFD; OpenFOAM

Для цитирования: Али Р. Влияние относительного продольного расстояния на динамическое поведение двух взаимодействующих судов при встречном волнении. Труды ИСП РАН, том 34, вып. 6, 2022 г., стр. 185-196. DOI: 10.15514/ISPRAS-2022-34(6)-15

1. Introduction

Nowadays, there is a significant increase in marine applications that involve ships floating in very close proximity. Lightering operations and ship-tug maneuvering are considered typical examples of such investment operations involving multibody floating systems. Being in the waves complicates the hydrodynamic interactions of such a system since each body experiences the incident waves in addition to the diffracted and radiated wave systems of another body, which may result in unfavorable responses and lead to dangerous scenarios. Therefore, studying the motion responses of such a multi-body system in waves is extremely important.

Chongwei Zhang [1] studied the hydrodynamic interaction between two identical barges, one of which was fixed and the other was allowed to sway freely in head waves; the obtained results indicated that amplitudes of the barge motion and maximum wave elevation in the gap generally increased with the reduction in the gap width. V. Yu. Semenova and Aung Myo Thant [2] studied the influence of lateral separation between ships on the damping and added mass coefficients for two interacting ships in shallow water. Zhi-Ming Yuan [3] developed a 3-D panel code based on the Rankine source method to investigate the hydrodynamic interaction between two ships in shallow water. Yuan studied the influence of the lateral distance between two Wigley III hulls on the RAO “Response Amplitude Operator”, and the obtained results indicated that the resonant frequency is greatly influenced by the gap between the ships. Yoshiyuki Inoue and Mir Tareque Ali [4] used the far-field approach to investigate the numerical accuracy of the computation of multi-body systems floating in deep water on regular waves. In their research, the numerical calculations were carried out for a parallelly connected FPSO “Floating Production Storage and Offloading” and LNG “Liquefied Natural Gas” carrier for different wave heading angles and for various separation distances between these ships. It was found that some of the motion results particularly roll and yaw motion exhibit considerable amount of deviation from the experimental one. Yoshiyuki Inoue and Mir Tareque Ali [5] extended their research using the 3-D source-sink method to study the hydrodynamic interactions and dynamic behavior of two rectangular barges freely floating in deep water. Effects of beam and head sea conditions were considered, the lateral distance between the barges had also been varied and its influence on the ship motions had been studied. Binbin Li [6] studied the hydrodynamic interaction of side-by-side ships under different wave headings. His work concentrated on the resonant characteristics of parallel and nonparallel configurations, and the obtained results indicated that the higher resonant mode shifts to a lower frequency in the nonparallel configuration.

Ohkusu [7] extended the classical solution for a single heaving circular cylinder to the case of two cylinders in a catamaran configuration. Faltinsen and Michelsen [8] used the panel method to simulate the wave effects on 3D floating bodies. The panel method was further extended for two independent bodies by van Oortmerssen [9]. Ali and Tryaskin [10,11] used the CFD “Computational Fluid Dynamics” method to investigate the hydrodynamic interaction of two bodies in deep water.

In this paper, the fluid flow around two close ships floating in close proximity on head waves in shallow water was simulated. A wide range of longitudinal spans were tested, and their effects on the frequency characters were obtained.

The paper starts by defining the problem in section 2, which includes a brief description of the geometrical and operational characteristics of the “Aleksey Kosygin” and “Novgorod” hulls in addition to the governing equations and turbulence modeling approaches. A detailed review of the computational domain, mesh specifications, numerical settings, and boundary conditions is described in section 3. Validation with experimental data is subsequently performed. Finally, results and discussion of the effects of relative longitudinal position on the frequency characters of two interacted ships are discussed in section 4, conclusions are presented in section 5.

2. Problem definition

2.1 Hull form

The ships under consideration are the lightering ship "Aleksey Kosygin" and the general cargo ship "Novgorod"; the displacement of both ships is 53000 tons and 17000 tons, respectively. In this study, two scaled models with a scale factor of k=0.0177 are used: the "Aleksey Kosygin" model plays the role of the ship to be lightered (STBL), while the "Novgorod" model plays the role of the service ship (SS). The hull shape and the principal dimensions and coefficients of both ships are shown in Table 1 and Fig. 1, respectively.

Table. 1. Main particulars of the "Aleksey Kosygin" and "Novgorod" ships

	LBP	*B*	*T*	*CB*
Aleksey Kosygin	*232.0*	*32.0*	*10.6*	*0.660*
Novgorod	*138.0*	*20.6*	*9.0*	*0.661*

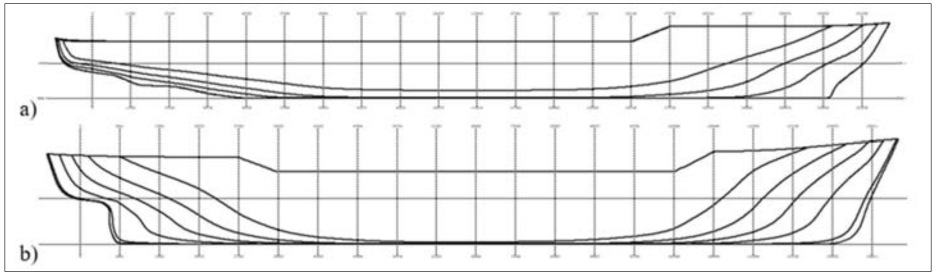

Fig. 1. Geometry of the interacting ships a) "Aleksey Kosygin" and b) "Novgorod "ships

2.2 Axis Conventions

Three sets of right-handed coordinate systems are used; an earth-fixed coordinate system S (x_0; y_0; z_0) with origin located at the still water surface and x_0 axis points to the direction of wave propagation, a fixed coordinate system O (x; y; z) linked to each ship, its origin is located at the intersection of the center-plane, midship plane, and water-plane, with X axis points to the ship bow, a body bounded coordinate system G (x_b; y_b; z_b) connected to the center of gravity G of each ship with x_b axis oriented to the ship bow.

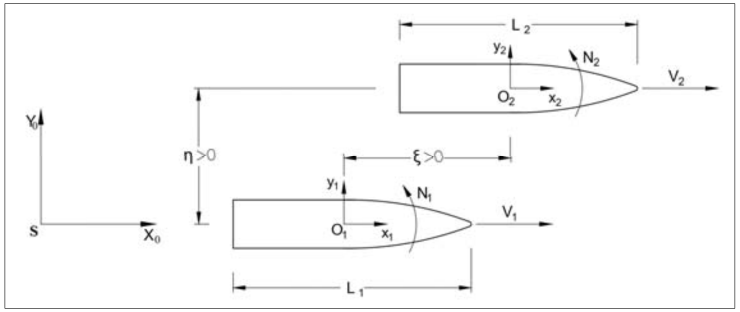

Fig. 2. Coordinate systems used for two interacting ships in waves

The vertical axes in all coordinate systems are directed upward. The fixed coordinate system is used to define the relative positions of each ship to another, as well as their linear and rotational motions. The corresponding right-handed coordinates are shown in Fig. 2.

2.3 The non-dimensionality terms

In this study, both ships float parallel on regular head waves without forward speed in shallow water $\frac{h}{T_{STBL}} = 1.8$, where h is the water depth [m]. The SS is always located at the starboard side of the STBL and its position is defined by the origin location of its fixed coordinate system in the STBL fixed coordinate system. To clearly describe the case and to reduce the number of variables associated with it, the relative position of the two ships is defined non-dimensionally as follows:

- The non-dimensional lateral distance (η), $\eta = dy/B_{avg}$ where dy is the lateral distance between the centerlines of the ships, B_{avg} is the average molded breadth of the SS and STBL;
- The non-dimensional longitudinal distance (ξ), $\xi = dx/L_{avg}$ where dx is the longitudinal distance between the mid-sections of the ships, L_{avg} is the average length between perpendiculars of the SS and STBL.

When the interacted ships float in symmetry position, their midship planes coincide and so the ξ=0.

The linear and rotational amplitudes of the heave, roll, and pitch motions of both ships will be computed and displayed in a dimensionless form as follows:

$$RAO_{heave} = \frac{F_3}{\zeta_a}, RAO_{roll} = \frac{F_4}{2\pi\zeta_a/L_{avg}}, RAO_{pitch} = \frac{F_5}{2\pi\zeta_a/L_{avg}}$$

where F_3, F_4 *and* F_5 are the model response in the corresponding direction, ζ_a is the amplitude of incident waves[m].

During the study, the lateral distance η was kept constant and equal to 1.3, while the longitudinal distance ξ was varied to cover the following values: 0%, 15%, 30%, 50%, and100%.

The longitudinal distance ξ is used to indicate the position of the SS relative to the STBL. So, the relative positions of SS are classified into two main categories: front and rear positions. In the front positions, the service ship SS is shifted forward compared with the symmetry position (alongside position), so the nondimensional longitudinal positions will have a positive value $\xi > 0$, while in the rear positions, the service ship SS is displaced oppositely, and so $\xi < 0$.

3. Governing Equations, Turbulence Model

Continuity and Navier–Stokes equations are the basic equations governing the fluid flow, to describe the turbulent of viscous fluids with a logical computational resource consumption, the Reynolds average is applied over the continuity and Navier–Stokes equations, PDEs of RANS are described as follow:

$$\frac{\partial \bar{u}_i}{\partial x_i} = 0, \tag{1}$$

$$\frac{\partial \bar{u}_i}{\partial t} + \bar{u}_j \frac{\partial \bar{u}_i}{\partial x_j} = -\frac{1}{\rho}\frac{\partial \bar{P}}{\partial x_j} + \vartheta \frac{\partial^2 \bar{u}_i}{\partial x_j \partial x_j} - \frac{\partial \overline{\acute{u}_i \acute{u}_j}}{\partial x_j} + g_i + F_{\sigma i} \tag{2}$$

where P is the pressure, u_i and g_i are the velocity and the gravitational acceleration components in the cartesian coordinate system, $\overline{\acute{u}_i \acute{u}_j}$ is Reynolds stress, ρ is the fluid density, ϑ is the kinematic viscosity and $F_{\sigma i}$ is the surface tension force.

The air-water interface is captured using the Volume of Fluid (VOF) method.

$$\frac{\partial \alpha}{\partial t} + \nabla \cdot (U\alpha) = 0 \tag{3}$$

where: α is the volume fraction, t denotes time, U is the fluid velocity.

RANS equations are closed with two equations $SST\ k{-}\omega$ turbulence model presented by Menter [12]. Menter Shear Stress Transport Turbulence Model $SST\ k{-}\omega$ is a two-equation eddy-viscosity model used for many hydrodynamic and aerodynamic applications, this model combines the well-known low Reynolds turbulence model $k{-}\omega$ and high Reynolds turbulence model $k{-}\varepsilon$, the former is suitable for simulating flow in the viscous sub-layer, while the latter is ideal for predicting flow behavior in regions away from the wall, the built-in blinder of $SST\ k{-}\omega$ ensures the appropriate use of these models. The most recent version of the $SST\ k{-}\omega$ model consists of the following formulas:

$$\frac{\partial(\rho k)}{\partial t}+\frac{\partial(\rho u_i k)}{\partial x_i}=P_k-\beta^*\rho k\omega+\frac{\partial}{\partial x_i}\left[(\mu+\sigma_k\mu_t)\frac{\partial k}{\partial x_i}\right], \tag{4}$$

$$\frac{\partial(\rho\omega)}{\partial t}+\frac{\partial(\rho u_i\omega)}{\partial x_i}=\alpha\rho S^2-\beta\rho\omega^2+\frac{\partial}{\partial x_i}\left[(\mu+\sigma_\omega\mu_t)\frac{\partial\omega}{\partial x_i}\right]+2(1-F_1)\rho\sigma_{\omega^2}\frac{1}{\omega}\frac{\partial k}{x_i}\frac{\partial\omega}{\partial x_i} \tag{5}$$

where k is turbulent kinetic energy, μ dynamic viscosity, μ_t eddy viscosity, P_k production of turbulent kinetic energy, ω specific dissipation rate, S is the invariant measure of the strain rate, $F_1$is a blending function and σ_k, β, β^*, σ_ω, σ_{ω^2} are closure coefficients.

4. Numerical Formulation

4.1 Computational Domain

During the study, a box-shaped domain was chosen to conduct the entire series of simulations. The boundaries of the domain were located in a way that coincided with the ITTC "International Towing Tank Conference" requirements for wave generation and absorption. CreatMesh.py, a home-built script, was used to prepare a structured hexahedral mesh and automate the procedure of adjusting the boundaries. During the grid creation, and to maintain the height of the propagating wave, 100 cells within the wavelength and 20 cells within wave height were adhered to.

For all the studied waves, the inlet and outlet patches were located at least at 2L and 5L, respectively, away from the nearest hull, as shown in Table 2. To simulate the shallow water case, the water phase was adjusted in a way that the criteria $h/\lambda < 1/2$ and $h/T \le 2$ were achieved. The domain width was extended laterally by 3L, the air phase extended to $3L$ from the still water-free surface, where L and T are length and draft of STBL, h is water depth, λ is wave length. A general view highlighting different zones of the computational domains is shown in Fig. 3.

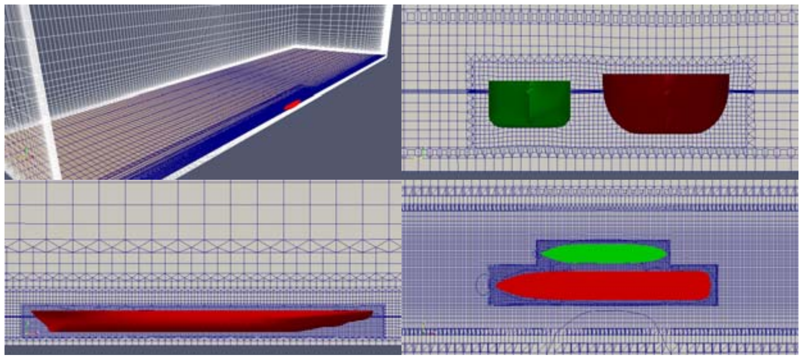

Fig. 3. Overview of computational domain and Grid structure around STBL and SS

Table 2. Inlet and outlet patches of the numerical wave tank

	$\lambda/L > 1$	$\lambda/L \le 1$
Inlet ahead of front ship	$0.5L + 2\lambda$	$2L + 0.5\lambda$
Outlet behind the rear ship	$2L + 2\lambda$	$3L + 3\lambda$

4.2 Numerical settings

For complicated fluid flows, FVM is used to discretize the PDEs of the governing equations over the domain. in order to minimize the consumption of the computational resource, the discretized form of PDEs of RANS were solved using OpenFOAM CFD package.

Wave generating, propagating and absorbing in the NWT "Numerical Wave Tank" were conducted by waveFoam solver. The time discretization is based on the first-order Euler bounded scheme, and the spatial discretization is performed with a linear second-order central differencing scheme for the convection and diffusion terms.

The simulation was treated as unsteady. PIMPLE, a pressure-velocity coupling algorithm based on the finite volume method, was used. Piso algorithm was launched by eliminating the outer correctors, and pressure fields were corrected twice for each time step. Courant number was limited to $CFL \le 0.25$, time step was left to OpenFOAM by turning on adjustTimeStep option. The total time of the simulation was adjusted to 12 wave periods. According to the results reported in [13], turbulence intensity Tu and eddy viscosity ratio μ_t/μ were set to 5 and 60, respectively.

The water condition was modeled as fresh water at 17°C, and the corresponding values of density ρ and kinematic viscosity nu are set to ρ=998.8 [kg/m^3] and 1.09×10^{-06} [m^2/sec], respectively.

The waveVelocity and waveAlpha boundary conditions set the values from respective wave models at the inlet of the CFD domain. No-Slip boundary condition was set to the stationary hull surfaces immersed in the viscous fluid. Pressure values on the walls were assumed to be fixed with zero gradients, and pressure equal to atmospheric pressure was set at the outlet of the flow domain. An appropriate wall functions for turbulent fields were set on hull surfaces.

5. Validations

To study the mesh convergence and investigate the discretization errors, three grids were created: a fine grid of 4265293 elements, a medium grid of 2760868 elements, and a coarse grid of 1461957 elements. In compliance with the requirements of wall functions, y+>30 has been adhered to for all grids. Smoothed grids have the same structural architecture, and cell sizes across subsequent grids are correlated according to a ratio of √2 in all domain regions; the cell-to-cell aspect ratio was kept at 1.2 in the stretching regions.

The heave RAO of the "Novgorod" vessel was evaluated on head waves using the three grids; the numerical results at wave period 2.79 seconds in model scale were compared with the published results of Semenova and Thant [2], and the relative error in the coarse, medium, and fine grids was 10.41%, 2.99%, and 1.07%, respectively. The true numerical solution was estimated using Richardson extrapolation and found to be 0.798. The grid convergence index (GCI%) was calculated for fine-medium grid and medium-coarse grid and found to be 0.83 and 3.15, respectively.

The grid numerical analysis indicates asymptotically approaching towards the converged solution. Based on the conducted study and to achieve a balance between computational accuracy and simulation time, the medium grid was chosen to perform the numerical simulation in this article.

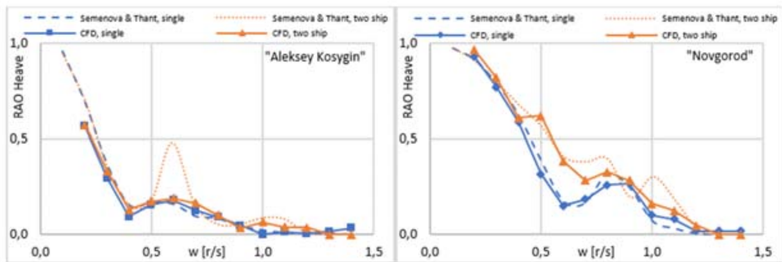

Fig. 4. Heave RAO for the two interacted ships, "Aleksey Kosygin" (left) and "Novgorod" (right)

However, Semenova and Thant's potential results for "Aleksey Kosygin" and "Novgorod" hulls, floating stationary on head waves and shallow water and located parallelly without longitudinal span at close lateral span η=1.3, were used as benchmarks to evaluate the CFD results [2].

The validations covered the heave RAO of a single ship as well as two interacting ships. The results of CFD simulations were illustrated in Fig. 4 against potential results, and they seem to be in good agreement which confirms the quality of the grid and the accuracy of the results obtained.

6. Results

The validation presented above provides a brief overview of the hydrodynamic interaction between two ships in close proximity; however, the frequency characteristics of two interacting ships are affected by their relative longitudinal positions. To clearly represent the results, the effect of the relative longitudinal position ξ on the ship's motions (heave, pitch, and roll) will be shown separately for each vessel, and a distinction will be made between the cases of forward and backward positioning of the SS with respect to the STBL. Calculations were performed for about two months on node of 20-cores, 3.00 GHz Intel Xeon CPU, 64 GB DDR3, Linux 4.19.0-21-amd64 (x86_64).

6.1 Effect of changing the relative longitudinal position on the heave motions of the interacting ships

Changing the relative longitudinal position ξ differently affects the amplitude of the vertical motions of each of the SS and STBL ships. It has a clear effect on the service ship SS, while its effect is limited on the STBL ship over the entire spectrum of the studied wave frequencies.

Fig. 5 and 6 show the effect of different relative longitudinal positions, including the symmetry position $\xi = 0$, on the heave motion of the two interacting vessels, SS and STBL.

The results obtained by the numerical simulation will be displayed and discussed according to the relative longitudinal position ξ of SS as follows:

6.1.1 Front positions

Figure 5 depicts the influence of SS forward positions on the heave's RAO of both SS and STBL.

For SS, the curves in Fig. 5 indicate that the effect of the forward positions on the heave motion is related to the wave frequency. The forward positions have a negligible effect at wave frequencies higher than $\omega = 1.2$ and a random effect within the frequency range $\omega \in [0.9,1.2]$. However, forward positions are beneficial and lead to a decrease in the heave motion, compared to symmetry position, at wave frequencies smaller than $\omega = 0.9$.

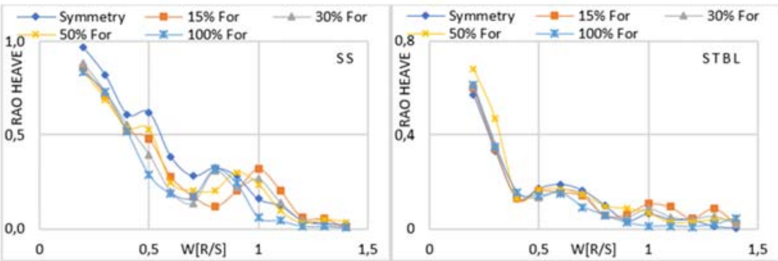

Fig. 5. RAO of heave motions for both SS and STBL ships at positive values of ξ

Changing the front longitudinal position of SS plays an effective role in reducing her vertical motions within the frequency range $\omega \in]0.4,0.9[$, while its effect is weak outside this range. The ability to reduce vertical motions by changing the forward relative position ranges from 14.8% at frequency 0.4 to 53.2% at frequency 0.5.

Regarding the STBL, the front positions of the service ship SS have a random negligible effect on the heave motion of the STBL. However, within the frequency range 0.5 to 0.8, the SS forward positions reduce STBL heave motions comparing to the symmetry position.

6.1.2 Rear positions

Shifting the SS backwards plays an effective role in reducing her vertical motion along a range of wave frequencies that extends from $\omega = 0.2$ to $\omega = 1.2$, Fig. 6.

The ability to reduce the SS vertical motions by altering her rear position ranges from 9.9% at frequency 0.4 to 53.8% at frequency 0.5.

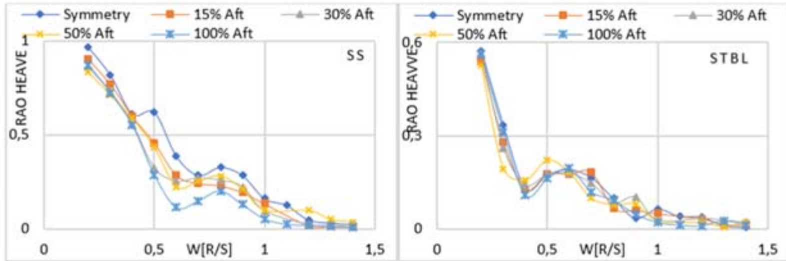

Fig. 6. RAO of heave motions for both SS and STBL ships at negative values of ξ

Regarding STBL, the rear positions of the service ship SS positively affect the vertical motions of the STBL for wave frequencies smaller than 0.4, while it has a random effect outside this range.

6.2 The effect of changing the relative longitudinal position on the pitch motions of interaction ships

The effect of the relative longitudinal position on the pitch motion was studied for two interacting ships floating stationary on head waves at a small transverse distance $\eta = 1.3$. The results are shown separately for front and rear positions in Fig. 7 and Fig. 8, respectively.

6.2.1 Front positions

The analysis of the numerical results shows that, in comparison with the symmetry position case, the forward position of the service ship SS slightly affects the pitch motions of each of the two interacting ships.

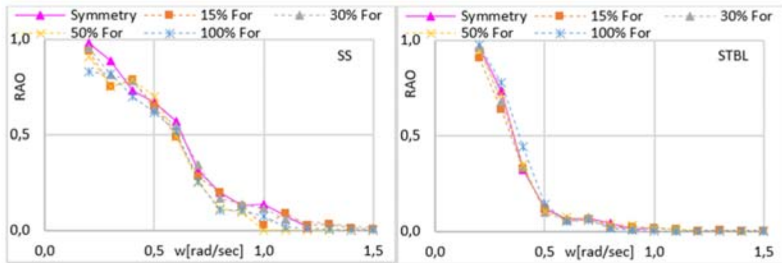

Fig. 7. RAO of Pitch motions for both SS and STBL ships at positive values of ξ

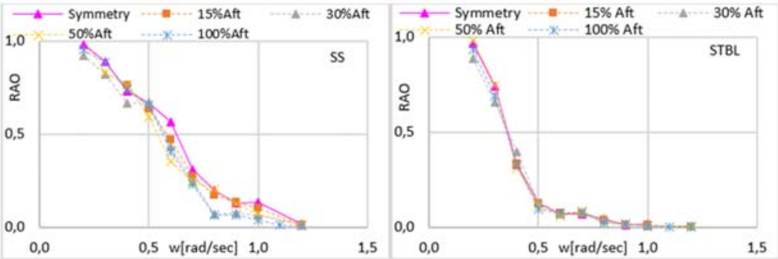

Fig. 8. RAO of pitch motions for both SS and STBL ships at negative values of ξ.

6.2.2 Rear positions

When it comes to rear positions, the curves presented in Fig.8 shows that, in comparison to the case of symmetry position $\xi = 0\%$, the rear positions of the service ship SS decrease her pitch motion while slightly affect the pitch motion of STBL. The positive effect of the rear position on the SS pitch motion appears clearly for wave frequencies that fall within the range $\omega \in [0.5, 1]$.

The curves of Fig. 8 confirm that a rear position of the service ship SS of $\xi = 50\%$ causes a reduction in her pitch motion by 11.4%, 37.9% and 21.5% for a wave frequency $\omega = 0.5,\ 0.6$ and 0.7 respectively.

6.3 The effect of changing the relative longitudinal position on the roll motions of interacting ships

6.3.1 Front positions

Forward positions of the SS reduce the peak of roll motion of both SS and STBL ship when compared to the case of symmetry position. An exception is the forward position $\xi = 30\%$, which is associated with an increase in the roll peak of the STBL by 19.3%, Fig. 9.

The curves in Fig. 9 confirm that the shift of the SS to a forward position greater than $\xi = 50\%$ causes a clear reduction in the values of the roll motions of both ships over the entire range of the studied wave frequencies.

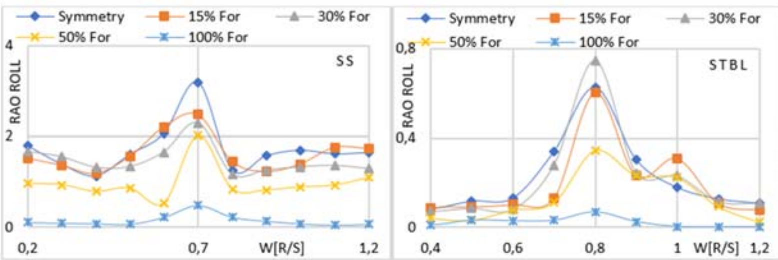

Fig. 9. RAO of roll motions for both SS and STBL ships at positive values of ξ.

In order to more clearly show the effect of the longitudinal position on the peak of roll motion, the change of peak values was represented in Fig. 11 as a function of the non-dimensional longitudinal position ξ for each ship.

Curves of Fig. 11 ensure that the forward relative longitudinal position $\xi \geq 50\%$ has a positive effect on both ships, $\xi = 50\%$ results in a 36.8% reduction in roll peak of the SS and 45% for the STBL.

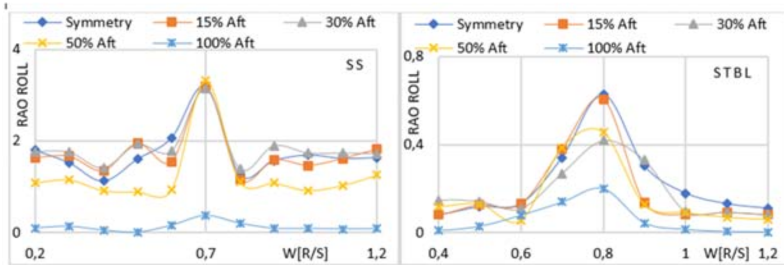

Fig. 10. RAO of roll motions for both SS and STBL ships at negative values of ξ.

6.3.2 Rear positions

Along a range of longitudinal positions extending from the symmetry position to $\xi = 50\%$ aft, the roll peak of the service ship SS showed a small influence, and its changes remained confined to the small range between -0.6% and 4% only. However, this is not the case for the STBL ship, where the relative longitudinal position $\xi = 30\%$ aft of SS is associated with a clear decrease in the STBL peak value up to 33%, Fig. 10 and Fig. 11.

Curves in Fig. 10 and Fig. 11 ensure that shifting the SS to a rear position $\xi > 50\%$ causes a clear and significant reduction in the roll motions of both ships.

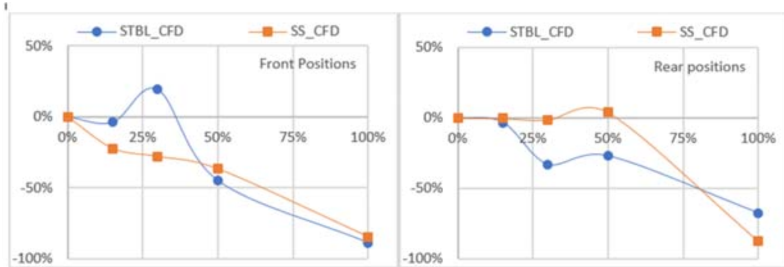

Fig. 11. The change of roll peak as a function of ξ for both SS and STBL

7. Conclusions and recommendations

OpenFOAM, an open-source CFD package, was used to simulate the motion response for two ships floating in close proximity in head waves and shallow water. RANS method was used for turbulence modeling and the well-known turbulent model k-ω SST was used to close RANS equations. The results of numerical simulation conducted on ships “Aleksey Kosygin” and “Novgorod” showed that the relative longitudinal position affects the RAO of the heave, pitch and roll motions of each of the two ships. The following results are obtained for ship length ratio 1.68, and lateral separations $\eta = 1.3$:

- The frequency characteristics of the ship motion are related not only to the frequency of the induced wave but also to the relative longitudinal position between the two ships.
- In general, the heave of STBL ship is less sensitive to the longitudinal change of position compared to the service ship SS. Shifting the service ship SS away from the symmetry position reduces her heave motion within the range of wave frequencies $\omega < 0.9$; maximum effectiveness takes place at frequencies $\omega \in]0.4, 0.9[$.
- Changing the SS longitudinal position has a neglected effect on the pitch motion of the STBL ship. The rear positions decrease SS pitch motion when compared with the symmetry position.

- Forward and rear positions $\xi > 50\%$ ensures a reduction in the peak of roll motions for both ships.

References / Список литературы

[1] Zhang C., Sun X. et al. Hydrodynamics of a floating barge adjacent to fixed structure in transient wave fronts. Physics of Fluids, vol. 33, issue 10, 2021, article id. 107106, 49 p.

[2] Semenova V.Yu., Thant A.M. The investigation of the influence of the distance between the ships and the fairway depth on the hydrodynamics characteristics of their joint motions in shallow water. Research Bulletin by Russian Maritime Register of Shipping, issue 44/45, 2016, pp. 61-68 (in Russian) / Семенова В.Ю., Тхант А.М. Исследование влияния расстояния между судами и глубины фарватера на гидродинамические характеристики их совместной качки на мелководье. Научно-технический сборник Российского морского регистра судоходства, вып. 44/45, 2016 г., стр. 61-68.

[3] Yuan Z.-M., Incecik A., He S. Hydrodynamic Interaction Between Two Ships Arranged Side by Side in Shallow Water.In Proc. of the International Conference on Offshore Mechanics and Arctic Engineering, 2014, paper no: OMAE2014-23325, 10 p.

[4] Inoue Y., Ali M.T. A study on numerical accuracy for the prediction of motion responses and drift forces of multiple floating bodies. Journal of the Society of Naval Architects of Japan, vol. 2002, issue 192, 2002, pp. 289-298.

[5] Ali M.T., Inoue Y. On hydrodynamic interaction between two rectangular barges floating side-by-side in regular waves. In Proc. of the International Conference on Mechanical Engineering, 2005.

[6] Li B. Multi-body hydrodynamic resonance and shielding effect of vessels parallel and nonparallel side-by-side. Ocean Engineering, vol. 218, 2020, article no. 108188, 23 p.

[7] Ohkusu M. On the heaving motion of two circular cylinders on the surface of a fluid. Reports of Research Institute for Applied Mechanics, vol. XVII, issue 58, 1969, pp. 167-185.

[8] Faltinsen O. and Michelsen F. Motions of large structures in waves at zero Froude number. In Proc. of the International Symposium on the Dynamics of Marine Vehicles and Structures in Waves, 1974, pp. 91-106.

[9] van Oortmerssen G. Hydrodynamic interaction between two structures, floating in waves. In Proc. of the 2nd International Conference on Behavior of Offshore Structures, 1979, pp. 339-356.

[10] Ali R., Tryaskin N.V. Study the influence of the relative position of two vessels moving in parallel on their hydrodynamic characteristics. Marine intellectual technologies, issue 50, part 4, 2020, pp. 59-65 (in Russian) / Али Р., Тряскин Н.В. Изучение влияния относительного взаимного расположения двух движущихся параллельно судов на их гидродинамические характеристики. Морские интеллектуальные технологии, вып. 50, часть 4, 2020 г., стр. 59-65.

[11] Ali R., Tryaskin N.V. Study the influence of ship length ratio on ship to ship interaction on moving in parallel on their hydrodynamic characteristics. Marine intellectual technologies, issue 4, part 2, 2021, pp. 63-72 (in Russian)/ Али Р., Тряскин Н.В. Изучение влияния соотношения длин двух параллельно движущихся судов на их гидродинамические характеристики. Морские интеллектуальные технологии, Морские интеллектуальные технологии, вып. 4, часть 2, 2021 г., стр. 63-72.

[12] Menter F.R., Kuntz M., Langtry R. Ten Years of Industrial Experience with the SST Turbulence Model. In Proc. of the 4th International Symposium on Turbulence, Heat and Mass Transfer, 2003, pp. 625-632.

[13] Ali R, Tryaskin N.V. Numerical study on effect of the turbulence initial conditions on transition flow over 2D airfoil. Trudy ISP RAN/Proc. ISP RAS, vol. 31, issue 6, 2019. pp. 203-214. DOI: 10.15514/ISPRAS-2019-31(6)-1.

Information about the author / Информация об авторе

Rami ALI is a Senior Lecturer of the Department of Hydroaeromechanics and Marine Acoustics. Research interests: Marin hydrodynamics, computational fluid dynamics, CFD simulation, fluid structure interactions.

Рами АЛИ – старший преподаватель кафедры гидроаэромеханики и морской акустики. Научные интересы: морская гидродинамика, вычислительная гидродинамика, CFD-моделирование, взаимодействие жидкость-структура.